Macro-modeling of Liquid Crystal Cell with VerilogA

Makoto Watanabe*
SONY Corporation, Japan
MakotoD.Watanabe@jp.sony.com

Keiichiro Ishihara
SONY Corporation, Japan
Keiichiro.Ishihara@jp.sony.com

Takeyuki.Tsuruma
SONY Corporation, Japan
Takeyuki.Tsuruma@jp.sony.com

Yasuhiko Iguchi
SONY Corporation, Japan
Yasuhiko.Iguchi@jp.sony.com

Yoshiharu Nakajima
SONY Corporation, Japan
Yoshiharu.Nakajima@jp.sony.com

Yasuhito Maki
SONY Corporation, Japan
Yasuhito.Maki@jp.sony.com

ABSTRACT

In this paper, a macro-model for liquid crystal cells including electrical and optical behaviors is presented. This kind of model is feasible due to the high potential of VerilogA in mixed technology modeling. Subsequently, to realize higher performance, ADMS model compiler is used to generate C code for implementation through Spectre®'s compact model interface (CMI). This macro-model enables the optimum design of liquid crystal displays (LCDs).

1. INTRODUCTION

In accordance with its maturity, the LCD market is facing ever increasing expectations for products with higher quality. We can often see the case that a high performance in many aspects (high contrast, fast response, low power consumption and compact shape, etc.) is requested at the same time. To provide competitive products into the market, optical and electrical characteristics of LCDs should simultaneously be optimized to the highest level. To attain this goal, a circuit simulation technology including the liquid crystal cell model has been desired for the LCD design. A liquid crystal cell behaves as a non-linear history-dependent capacitor from the electrical point of view, and as a light valve the transmittance of which can be varied with the applied voltage from the optical point of view.

In the conventional design, the characteristics for a liquid crystal cell can be estimated with dedicated tools independent of circuit simulators. In such tools, the general algorithm is that the optical and electrical behavior can be estimated after the orientation of the liquid crystal molecule is determined by solving Poisson equations and Euler-Lagrange equations simultaneously with the iterative way. There already exists some commercial products[1] [2] [3] employing the manner above. As can be easily speculated, this method takes much time despite its high accuracy and is not suitable to be implemented into circuit simulators. From this background, a macro-model for a liquid crystal cell suitable for circuit simulators has been strongly demanded. However the established model already implemented into circuit simulators does not exist so far, although some models have been proposed in the past[4] [5] [6].

In this paper, we have enhanced Smet's approach[6] to improve the accuracy. The macro-model has been developed by the high level language VerilogA, which is reputable for the flexibility it provides in various kinds of fields. Furthermore, ADMS model compiler has been used for its implementation into Spectre® on Cadence Virtuoso® platform to achieve much higher performance considering the actual LCDs' structure which have millions of arrayed liquid crystal cells.

In section 2, a general dynamics of liquid crystal cell is introduced first. Next the macro-model proposed by Smet is reviewed and the enhancements by authors are described. The code in VerilogA and the implementation method with ADMS are shown in section 3. The model is evaluated and discussed for validity and performance in section 4. The application to LCD design of the model is illustrated in section 5. The paper is concluded in section 6 followed by an appendix.

2. MODELING OF LIQUID CRYSTAL CELL

2.1 Device

As shown in Figure 1, the typical liquid crystal cell consists of liquid crystal molecules aligned between two alignment layers, two electrodes, two glass substrates, polarizer, and analyzer. d in Figure 1 is the thickness of the liquid crystal layer. The alignment layers force the molecules to line up parallel to the substrates.
When a voltage is applied between the electrodes, a torque forces liquid crystal molecules to align parallel to the electric field $\boldsymbol{E}$. This changes the state of the polarization of incident light since the liquid crystal material is birefringent. Then the amount of the light that could pass the analyzer changes. By controlling the voltage applied to two electrodes, the amount of light transmitted through the cell can be varied.

*Mobile Display Business Group, Sony Corporation, 4-14-1 Asahi-cho, Atsugi, Kanagawa 243-0014, Japan

978-1-4244-1567-0/07/$25.00 (c) 2007 IEEE

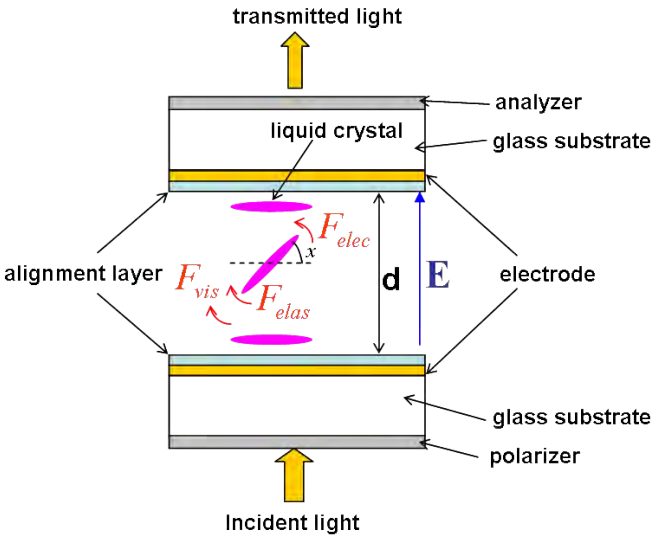

Figure 1: Schematic diagram of a liquid crystal cell

2.2 Macro-modeling

2.2.1 *Review of Smet's macro-model*

Here we review the macro-model proposed by Smet[6]. Through the review process below, authors dared to change the shape of equations slightly from the original ones for readers' easy understanding.

The average orientation of liquid crystal molecule is assumed to be represented by one-dimensional variable 'x' as shown in Figure 1. In practice, three kinds of torques are in play (see Figure 1).

(1) The elastic torque $F_{elas} = Kx(K : constant)$
This torque pulls the molecules back to their resting position x=0 (parallel to the alignment layer). This torque is assumed to follow Hooke's law.

(2) The electrical torque $F_{elec} = \mathrm{c\ E}^2(c : constant)$
This torque aligns the molecules parallel to the field $\boldsymbol{E}$. It is proportional to E^2.

(3) The viscosity torque $F_{vis} = \gamma\frac{dx}{dt}(\gamma : constant)$
This torque hinders any movements and is proportional to the velocity at which the molecules move.

Since the moment of inertia of liquid crystal molecule is small, it can be neglected. The equilibrium of torques in Figure 1 states that:

$$cE^2 = Kx + \gamma\frac{dx}{dt} \tag{1}$$

This is well-known first-order system with time constant $\tau = \gamma/K$ and $x(t) \to \frac{c}{K}\left[\frac{V_{ext}}{d}\right]^2 (t \to \infty)$. According to Smet's method, equation (1) is solved with low pass filter circuit shown in Figure 2. The resistance R_d and the capacitance C_d should be determined so that their product corresponds to the time constant $\tau = \gamma/K$. Note that the amount of electric field E in the cell is described as V_{ext}/d. Here V_{ext} and d are the applied voltage between two electrodes and the cell gap in Figure 1 respectively. After solving for x(t) from this circuit, the effective voltage V_i at time t is calculated by $V_i = \sqrt{\frac{Kd^2}{c}x(t)}$.

The static behaviors for the capacitance and transmittance of liquid crystal cells can be expressed empirically with equation (2) and (3) as a function of the effective applied voltage V_i.

$$C(V_i) = C_\perp + \frac{2}{\pi}(C_\parallel - C_\perp)\arctan\left[\frac{\alpha + (\alpha^2 + \delta^2)^{\frac{1}{2}}}{2}\right] \tag{2}$$

$$\alpha = \frac{V_i - V_{tc}}{V_{mc}}$$

$$T(V_i) = T_{min} + (1 - T_{min})\tanh\left[\frac{\beta + (\beta^2 + \eta^2)^{\frac{1}{2}}}{2}\right] \tag{3}$$

$$\beta = \frac{V_i - V_{to}}{V_{mo}}$$

$C_\parallel, C_\perp, \delta, V_{tc}, V_{mc}$ in equation (2) and $T_{min}, \eta, V_{to}, V_{mo}$ in equation (3) are treated as model parameters extracted in section 3.

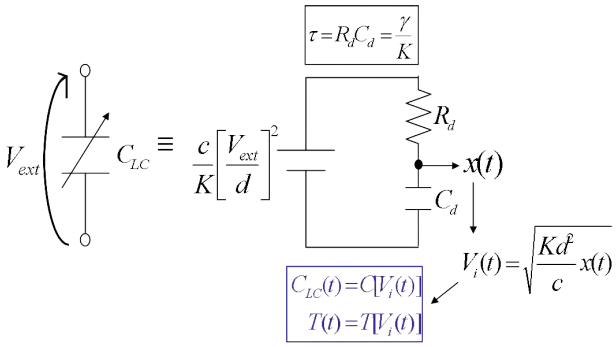

Figure 2: macro-model for Liquid Crystal Cell[6]

2.2.2 *Enhancements to improve accuracy*

To improve the accuracy, we have modified the form of the time constant(τ) in the equation proposed by Smet by considering the following points.

(1) External applied voltage dependency
Generally, the response time of liquid crystal depends on the external applied voltage(V_{ext}). We've got the following expression for time constant(τ) after further investigating of the relationship for the electric torque(F_{elec}) and the applied voltage(V_{ext}).

$$\tau = \frac{1}{a_1 + a_2 V_{ext}^m} \tag{4}$$

Here a_1, a_2, m are model parameters. Basically, m takes the value around 2. Explanation and deviation of equation (4) can be found in Appendix.

(2) Individuality of rise/fall process
The rise/fall process is defined as the case that the orientation angle x of the liquid crystal molecule is increasing/decreasing respectively. The time constant

for each process does not coincide generally. To implement this factor into our model, the parameters in equation (4) is selected after the voltage for both terminals of R_d are compared as below.

$$
\begin{aligned}
&if \\
&\qquad \frac{c}{K}\left(\frac{V_{ext}}{d}\right)^2 \geq x(t) \\
&then \\
&\qquad a_1 = a1\_r,\ a_2 = a2\_r \quad (for\ rise\ process) \\
&else \\
&\qquad a_1 = a1\_f,\ a_2 = a2\_f \quad (for\ fall\ process)
\end{aligned}
$$

This additional routine made the individual control of rise and fall behavior possible.

3. IMPLEMENTATION

3.1 Coding in VerilogA

We chose VerilogA language for describing our macro-model taking its advantage for flexibility and simple implementation into circuit simulators. Listing 1 shows an excerpt of the electrical property block of VerilogA code which stands for the non-linear history dependent capacitance. The block for the optical property is omitted here, but its algorithm is basically similar to the electrical one. For simplicity, $\frac{c}{Kd^2}$ in Section 2 is taken as 1. This substitution is always valid since it does not affect the result at all.

In Lines 3-6, the module for the capacitor with two interface ports `a` and `b` is defined. The node declared as `nvc` is the internal node in the low pass filter introduced in Section 2.

In Line 14, the initial orientation can be given as the amount corresponding to the effective applied voltage `vini`, since the orientation of liquid crystal molecule is not always 0 at the initial time (t=0).

In Lines 18-20, external voltage applied to the terminal of a capacitor is probed.

In Lines 22-32, whether the process is rising or falling can be judged by comparing both terminal voltages of the resistance in the low pass filter. The corresponding model parameter should be selected.

In Line 34, the amount of resistance which determines the time constant(τ) is computed from the external voltage and model parameters.

In Lines 36-39, the internal node voltage `V(nvc)` in the low pass filter is calculated. Note that this circuit is only used for the evaluation of the liquid crystal orientation and should not behave as the load of the actual external circuit.

In Lines 41-46, the capacitance for the liquid crystal cell is computed from the effective applied voltage `vrms_c`.

In Lines 48-50, the current flowing into the capacitor is feed backed into the external circuit.

Listing 1: Liquid Crystal Cell model in VerilogA.

```
1  // VerilogA for Liquid Crystal Capacitor
2  `include "discipline.h"
3  module lccap(a,b);
4  inout a,b; //Interface ports
5  electrical a,b;
6  electrical nvc; //Internal node
7                  ...
8  analog
9  begin
10  @(initial_step)
11    begin
12                 ...
13 //Initial voltage for internal node
14     vi_c = vini * vini;
15 end
16
17 begin
18 //Probing terminal voltage
19  vin = V(a,b);
20  vv = vin * vin;
21
22 //Detection of rising or falling
23   if (vv >= vi_c)
24    begin //rising
25      a1c = a1c_r;
26                 ...
27    end
28   else
29    begin //falling
30      a1c = a1c_f;
31                 ...
32    end
33 //
34  rdc = 1/(a1c + a2c * pow(vin, mc) );
35
36 // Calculation of Internal node voltage
37  I(nvc) <+ ddt(cdc * V(nvc));
38  I(nvc) <+ (V(nvc)-vv)/rdc;
39  vi_c = V(nvc);
40 //
41  vrms_c = sqrt(vi_c);
42  alpha = (vrms_c - vtc)/vmc;
43
44 // Capacitance calculation
45 cap = scale * area * (cv + cdiff * atan((alpha
46       +sqrt(alpha * alpha + delta * delta ))/2));
47
48 // Description for device behavior
49 qlc = cap * vin;
50 I(a,b) <+ ddt(qlc);
51
52   end
53  end
54 endmodule
```

3.2 Compilation with ADMS and CMI

Considering that millions of liquid crystal cells are arrayed in an actual LCD device, the performance of the native VerilogA module should not be sufficient. In order to achieve much higher performance, ADMS model compiler[7] has been used for its implementation into Spectre® on Cadence Virtuoso® platform.

A part of the code in native VerilogA(Listing1) should be modified so as to follow the syntax supported by ADMS[8]. The versions of ADMS and XML scripts used in this work is 2.2.4 and 2.1.1. respectively. ADMS is provided by Dr.Laurent Lemaitre and XML scripts by Cadence.

This methodology is so beneficial since it provides much higher performance and also keeps the confidentiality of device models, since this implementation method can be carried out inside the device manufacturing company without disclosing it to EDA vendors.

3.3 Model Parameters Extraction

We have 9 model parameters for static characteristics and 8 model parameters for dynamic one. To extract these parameters from the experimental data, we first roughly fit them on the spread sheet and next accurately fit them with the optimization tool Neocircuit® produced by Cadence. Neocircuit® optimizes parameters with the Genetic Algorithm (GA). This 2-step procedure maintains the high accuracy and saves time for extraction parameters at the same time.

4. MODEL EVALUATION

4.1 Validity

In this section, to verify the validity of the macro-model, results from the macro-model are compared with the experimental data.

4.1.1 Static behavior

Figure 3 shows the comparison of modeled and experimental data for the static behavior . The experimental data is measured in the twisted-nematic liquid crystal cell with $3.5\mu m$ gap. The model exhibits good agreement with the experimental data in both transmittance and dielectric constant characteristics.

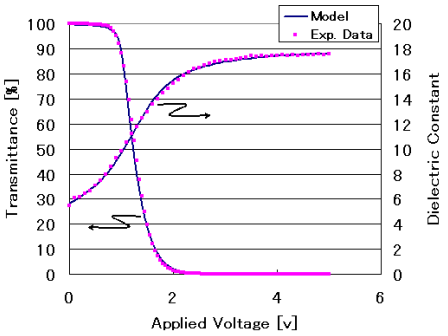

Figure 3: Comparison of static behavior between experimental data and the model

4.1.2 Dynamic behavior

Figure 4 and 5 show comparisons of modeled and experimental data for the dynamic behavior in some external applied voltages. The transient behavior from low voltage to high voltage(rising process) is shown in Figure 4. The transient behavior from high voltage to low voltage(falling process) is shown in Figure 5. Transient behavior for dielectric constant is not provided here because no measuring procedure is established so far. We have assumed that the dynamic parameters for transmittance and dielectric constant are same when this model is used in the actual design for the liquid crystal cell, though this assumption cannot be verified directly. In Figure 4 and 5, the model exhibits good agreement with the experimental data except for the following points.

(1) The bounce around 5msec in 3.30 → 0V in Figure 5

This phenomenon is well known as the back-flow of liquid crystal molecule[9]. This shape of the curve could not be expressed in principle since equation (3) is monotonous function. The new model supporting this phenomenon should be presented in the future.

(2) The disagreement after ample time in Figure 4 and in initial state in Figure 5

The origin of this disagreement is considered to be the measurement error, since the transmittance after ample time has passed in Figure 4 and in initial time in Figure 5 do not coincide with the ones in static measurement in Figure 3. It is hard to improve the measurement accuracy because the transmittance is very sensitive to the applied voltage around 1V as seen in Figure 3.

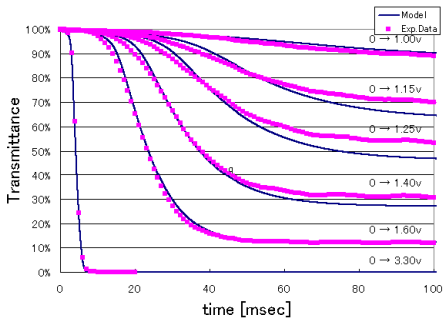

Figure 4: Dynamic behavior for rising process

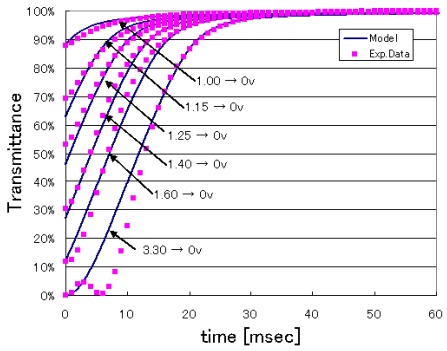

Figure 5: Dynamic behavior for falling process

4.2 Performance

We compared the elapsed cpu time in the circuit simulation among the following three models: (1)Compiled model with ADMS and CMI (2)Native VerilogA model (3)Physical model[1] introduced in Section 1. The result is shown in Figure 6. The compiled model with ADMS and CMI is 10 times faster than the native VerilogA model, and 500 times faster than the conventional physical model. This simulation is executed under the condition that 720 liquid crystal cells are arrayed and the transient time is set to 200msec. This bench mark test was carried out on a Linux server with 3.2GHz Intel® Xeon^{TM} processor, and 4GB of memory.

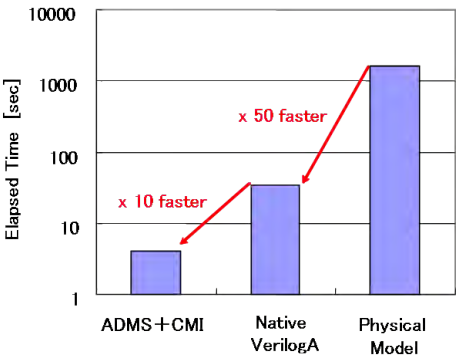

Figure 6: Comparison of performance

[1]Physical model is described in C-language and implemented into Spectre® with Spectre® CMI

5. APPLICATION TO LCD DESIGN

In this section, three examples of applying our macro-model to LCDs design are shown after the brief explanation of general LCDs operation.

In what follows, we describe briefly the principle of operation of an active matrix LCDs[10]. Figure 7(a) is a schematic diagram of a thin film transistor(TFT) array circuit for the active-matrix addressing of LCD. A detailed electrical pixel element of each pixel area is shown in Figure 7(b). We note that each pixel element has a TFT, a LC capacitor(C_{LC}), and a storage capacitor(C_{SC}). C_{LC} is dependent on the applied voltage as modeled in this paper. On the other hand, C_{SC} is a static capacitor.

When a gate line is addressed by V driver, a positive voltage is applied to the line turning on the TFT along the row. The TFT act as switches transferring electrical charges to the C_{LC} and C_{SC} from respective signal line connected to H driver. When addressing other rows, a negative voltage is applied to the gate lines turning off all the TFTs along the line and holding the electrical charges in C_{LC} and C_{SC} for one frame time until the line is addressed again. The DC voltage V_{COM} is applied to the storage line and one terminal of C_{LC} by the Vcom driver. To avoid the ionic material concentration on a surface, it is desirable to use AC voltage to drive the liquid crystal. This is achieved by switching the polarity of the signal line voltage in alternate frames.

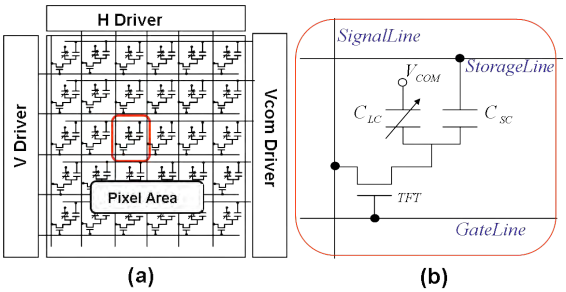

Figure 7: (a)Schematic drawing of TFT array circuit for LCD; (b)Electrical circuit diagram of one pixel element

5.1 Storage Capacitor (Csc) Optimization

C_{LC} and C_{SC} is charged to a signal line voltage V_{sig} at the end of TFT switched-on period. The electric field in the cell will then start to align the liquid crystal molecules so that the average dielectric constant changes. As a consequence, the value of C_{LC} also changes. But as the capacitor is isolated during TFT switched-off period, the total charge $Q = (C_{LC}+C_{SC})V_{sig}$ remains the same. This means that the effective voltage $V_{eff} = Q/(C_{LC}+C_{SC})$ will decrease/increase until the steady state is reached. By this V_{eff} modulation we cannot get obtain desired characteristics unless C_{SC} is large enough compared with C_{LC}. Figure 8 shows the optical transient behavior dependencies on C_{SC}. In this example, C_{LC} is 65fF at t=0 and 120fF in the steady state. In Figure 8, more than 200fF of C_{SC} is necessary for the high-speed response and obtaining the targeted transmittance (45%).

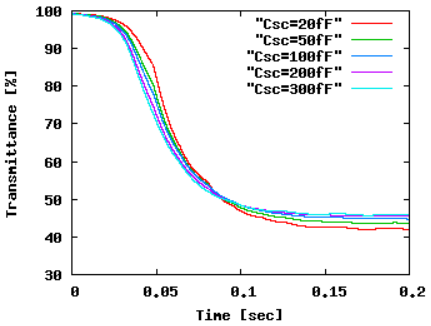

Figure 8: Optical response dependency on Csc

5.2 Vcom Optimization

As stated, the polarity of the signal line voltage is switched in alternate frames in general LCDs. The difference in the transmittance in alternate frames induces the flicker image and degrades the display quality. The transient transmittance vibration dependencies on V_{com} is shown in Figure 9(a). An optimum V_{com} setting (=3.4v) can drastically reduce the flicker as shown in Figure 9(a). Figure 9(b) has been acquired by taking the Fourier transformation of curves from 0.2 sec to 0.3 sec in Figure 9(a). The amount of level at 30Hz, corresponding to half of the frame rate of LCDs, is the main source of the flicker. The flicker phenomenon is known to be recognized when the level at 30Hz is over -20dB when taking its standard point at DC level(0Hz). This result suggests that V_{com} should be set within 3.4 ± 0.1v.

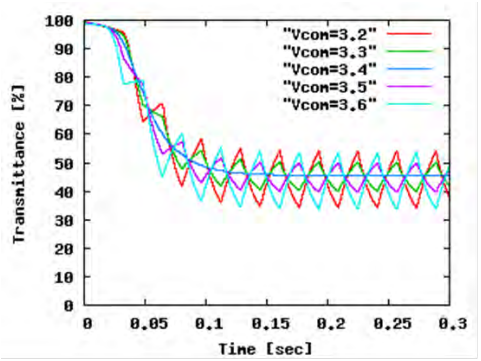

(a)

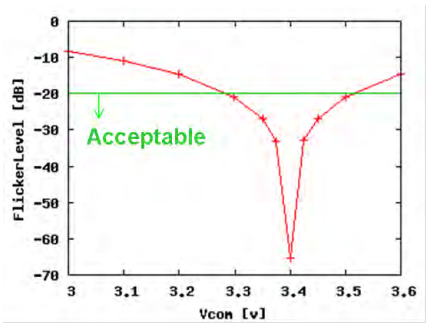

(b)

Figure 9: (a)Flicker phenomenon in LCDs; (b)Flicker level dependency on Vcom

5.3 Signal voltage design for each gray level

The relationship between the gray level and the transmittance is generally given by customers as one of specifications for LCDs. Our macro-model can also estimate the voltage to be applied to signal lines for each gray levels in order to obtain the proposed curve as shown in Figure 10. In this simulation, the transmittance has been averaged in the time frame from 200msec to 300msec. The transmittance here is basically different from the ones in Figure 4 and 5 in the point of including the modulation factors such as TFT's switching ability, the pulse distortion by the coupling noise from other signal lines, and the pulse delay on account of the parasitic capacitances and resistances.

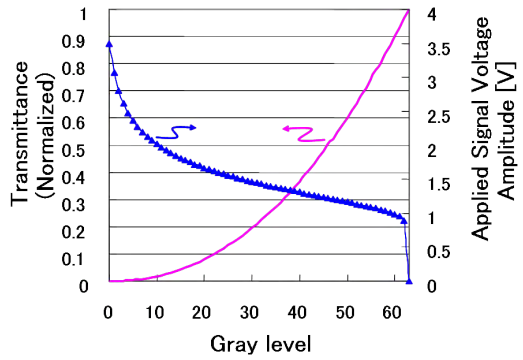

Figure 10: Signal voltages to obtain optimum transmittance for each gray levels

6. CONCLUSION

This paper describes the VerilogA modeling of a liquid crystal cell, taking advantage of the language to model multi-technological aspects of the module; optical and electrical. Subsequently, ADMS model compiler is used to generate C code for implementation through Spectre® compact model interface(CMI). With ADMS, the performances improved drastically; 10 times faster than the native VerilogA model, and 500 times faster than the conventional physical model. The validity of the implemented macro-model has been verified by checking the agreement with measurement data. The circuit simulation with this macro-model provides useful information for the optimum design of liquid crystal displays(LCDs).

7. ACKNOWLEDGEMENT

The authors wish to thank Dr.Laurent Lemaitre and Cadence for helpful advice and discussion when implementing our model into Spectre® on Cadence Virtuoso® platform.

8. REFERENCES

[1] http://www.autronic-melchers.com.
[2] http://www.daouxilicon.co.kr/davan/main.
[3] http://www.shintech.jp/eng/index.html.
[4] T.Shima. Liquid-crystal display cell model using piecewise approximations. *Electronics and Communications in Japan, Part II: Electronics*, 79(3):73–81, 1996.
[5] Hitoshi Aoki. Dynamic characterization of a-si tft-lcd pixels. *IEEE TRANSACTION ON ELECTRON DEVICES*, 43(1):31–39, Jan. 1996.
[6] Herbert De Smet. Electrical model of a liquid crystal pixel with dynamic, voltage history-dependent capacitance value. *Liquid Crystal*, 31(5):705–711, May 2004.
[7] L.Lemaitre. Adms - automatic device model sythesizer. In *Proc. IEEE Custom Int. Circ. Conf.*, pages 27–30, 2002.
[8] http://sourceforge.net/projects/mot-adms/.
[9] C.Z.van Doom. Dynamic behavior of twisted nematic liquid-crystal layers in switched fields. *Journal of Applied Physics*, 46(9):3738–3745, Sep. 1975.
[10] Pochi Yeh. *Optics of Liquid Crystal Displays*. John Wiley Sons, Inc., 1999.

APPENDIX

In this appendix, we derive the form of the voltage dependent time constant shown in equation(4).
$\boldsymbol{n}(|\boldsymbol{n}|=1)$ is director vector of liquid crystal. The director vector $\boldsymbol{n}$ roughly denotes the averaged orientation of the liquid crystal molecules. $\boldsymbol{E}$ is the electric field in the cell. As easily derived, the projection of $\boldsymbol{E}$ parallel to $\boldsymbol{n}$ is $(\boldsymbol{E},\boldsymbol{n})\boldsymbol{n}$ and perpendicular to $\boldsymbol{n}$ is $\boldsymbol{E}-(\boldsymbol{E},\boldsymbol{n})\boldsymbol{n}$ respectively. Therefore the displacement field vector $\boldsymbol{D}$ can be written as in equation (5). Note that the dielectric constants of liquid crystal differs in value along the parallel to the axis($\epsilon_\parallel$) and perpendicular to the axis($\epsilon_\perp$).

$$\boldsymbol{D}=\epsilon_0[\epsilon_\parallel(\boldsymbol{E},\boldsymbol{n})\boldsymbol{n}+\epsilon_\perp\{\boldsymbol{E}-(\boldsymbol{E},\boldsymbol{n})\boldsymbol{n}\}] \tag{5}$$

In this case, the electromagnetic energy density U can be written in equation(7).

$$U = -\frac{1}{2}\epsilon_0(\boldsymbol{E},\boldsymbol{D}) \tag{6}$$

$$= -\frac{1}{2}\epsilon_0[(\epsilon_\parallel-\epsilon_\perp)(\boldsymbol{E},\boldsymbol{n})^2+\epsilon_\perp|\boldsymbol{E}|^2] \tag{7}$$

Here z-axis is parallel to $\boldsymbol{E}$, θ is the angle between $\boldsymbol{n}$ and z-axis, and ϕ is the angle between the projection vector of $\boldsymbol{n}$ into x-y plane and x-axis. $\boldsymbol{E}$ and $\boldsymbol{n}$ are expressed as $\boldsymbol{E}=(0,0,E_z)$, $\boldsymbol{n}=(\cos\theta\cos\phi,\cos\theta\sin\phi,\sin\theta)$, then equation (8) can be derived from equation (7).

$$U=-\epsilon_0(\epsilon_\parallel-\epsilon_\perp)E^2(\epsilon_\parallel\sin^2\theta+\epsilon_\perp\cos^2\theta)+\epsilon_\perp E_z^2 \tag{8}$$

Applied torque to director by the electric field is shown in equation(10).

$$f = -\frac{\partial U}{\partial\theta} \tag{9}$$

$$= \frac{1}{2}\epsilon_0(\epsilon_\parallel-\epsilon_\perp)E^2\sin(2\theta) \tag{10}$$

Under the assumption that $\sin\theta\approx\theta$ when θ is very small,

$$f=\epsilon_0(\epsilon_\parallel-\epsilon_\perp)E^2\theta \tag{11}$$

For the convenience, the dielectric anisotropy $\Delta\epsilon$ is defined as $\Delta\epsilon\equiv\epsilon_\parallel-\epsilon_\perp$. Then,

$$f=\epsilon_0\Delta\epsilon E^2\theta \tag{12}$$

When equation (12) replaces the electrical term in equation(1), torque balance equation(1) can be rewritten by equation(13).

$$\epsilon_0\Delta\epsilon E^2\theta = K\theta+\gamma\frac{d\theta}{dt} \tag{13}$$

$$\frac{d\theta}{dt} = \left(\frac{\epsilon_0\Delta\epsilon E^2-K}{\gamma}\right)\theta \tag{14}$$

Therefore the time constant for equation(14) can be expressed as follows.

$$\tau = \frac{\gamma}{\epsilon_0\Delta\epsilon E^2-K} \tag{15}$$

$$= \frac{1}{\left(\frac{\epsilon_0\Delta\epsilon}{\gamma}\right)\left(\frac{V}{d}\right)^2-\left(\frac{K}{\gamma}\right)} \tag{16}$$

$$\equiv \frac{1}{a_1+a_2V^2} \tag{17}$$